

# INTERNATIONAL SOCIETY FOR SOIL MECHANICS AND GEOTECHNICAL ENGINEERING



*This paper was downloaded from the Online Library of the International Society for Soil Mechanics and Geotechnical Engineering (ISSMGE). The library is available here:*

<https://www.issmge.org/publications/online-library>

*This is an open-access database that archives thousands of papers published under the Auspices of the ISSMGE and maintained by the Innovation and Development Committee of ISSMGE.*

*The paper was published in the proceedings of the 7<sup>th</sup> International Conference on Earthquake Geotechnical Engineering and was edited by Francesco Silvestri, Nicola Moraci and Susanna Antonielli. The conference was held in Rome, Italy, 17 - 20 June 2019.*

# Evaluation of strain dependent shear modulus and damping ratio of unsaturated silty soil during drying path with resonant-column-torsional shear

S. Banar & S.M. Haeri

*Department of Civil Engineering, Sharif University of Technology, Tehran, Iran*

A. Khosravi

*Department of Civil and Environmental Engineering, University of California Davis, Davis, CA, USA*

M. Khosravi

*Department of Civil Engineering, Montana State University, Bozeman, MT, USA*

**ABSTRACT:** This paper describes the details, experimental procedure, and results of a resonant column torsional shear test device to evaluate changes in the strain-dependent shear modulus and damping ratio of an unsaturated silt during drying (matric suction increase). The testing device employed in this study uses the axis translation technique for suction control and is capable of measuring  $G$  and  $D$  at strain levels ranging from  $10^{-5}$  to  $10^{-3}$  at different matric suctions and mean net stresses, the two unsaturated stress state variables. For a compacted silt tested under a constant mean net stress, shear modulus was found to increase during drying, while damping ratio decreased as matric suction was increased. Results of the study were also used to calibrate a conventional shear modulus reduction curve that is well calibrated for saturated soils at small-to-moderate shear strains.

## 1 INTRODUCTION

Many geotechnical systems involve unsaturated soils. These soils experience both cyclic loading and seasonal variations which cause significant changes in their matric suction over time (e.g., pavements). A rational framework for analysis has not yet been developed for assessment of the effects of these important variables on the development of plastic strain during cyclic loading. It is the view of the authors that studies in this area have been restrained by the lack of advances in both the definition of the effective stress state in unsaturated soils, and in the lack of measurements of dynamic properties of unsaturated soils. Based on Mancuso et al. (2002), Khosravi & McCartney (2011), Khosravi & McCartney (2012), Khosravi et al. (2016), and Dong et al. (2016), the trends in the dynamic properties of unsaturated soils (e.g. secant modulus and damping ratio) with stress state may be significantly different from those observed for saturated soils. The inter-particle contact forces in unsaturated soils arising from the effects of matric suction are expected to lead to an increase in the dynamic shear and compression moduli, and a decrease in the damping coefficient. Accordingly, the matric suction in unsaturated soils is expected to lead to a greater resilience to plastic strain development during cyclic loading than what is expected for the same saturated soils.

Previous studies on the effect of unsaturated stress state variables on dynamic properties of unsaturated soils have mainly focused on the effects of matric suction and net stress on the shear modulus of unsaturated silt (Khosravi and McCartney 2011, Khosravi and McCartney 2012, Hoyos et al 2015, Khosravi et al. 2016) and sand (Khosravi et al. 2010, Khosravi et al. 2018) at small strains. Results of these studies indicated that at small strain, depending on the

soil type, an increasing (for silt) or up-and-down trend (for sand) could be observed for the shear modulus with increasing matric suction. The limited experimental data, however, do not provide sufficient information to quantify unique and clear trends for these parameters at large strain (Biglari et al. 2011, and Ghayoomi et al. 2017).

This paper summarizes results of a series of element-scale tests at large strains examining the impacts of stress state and strain level on the dynamic behavior of unsaturated soils. A combined resonant column torsional shear test device (RCTS) was adapted for unsaturated soil testing and used to determine the dynamic shear modulus and damping ratio at small and large strains. This device has been extensively used in the past for characterization of the dynamic properties of saturated, dry (Hardin & Black 1968, 1969; Stokoe et al. 1999) and unsaturated soils (Khosravi & McCartney 2011, Khosravi & McCartney 2012, Hoyos et al 2015, Khosravi et al. 2016). The tests were conducted by controlling the unsaturated stress state using the axis-translation technique (Hilf 1956). An improved understanding of the dynamic response of unsaturated soils is expected to lead to improved accuracy of design efforts for deformation prediction of geotechnical systems like pavements and machine foundations.

## 2 EXPERIMENTAL PROCEDURES

### 2.1 Materials

A non-plastic silt is used in this study. The grain-size distribution of the silt is shown in Figure 1(b). Properties of the non-plastic silt include the following: specific gravity of solids,  $G_s = 2.65$ ; dry density,  $\rho_d = 1.4 \text{ gr/cm}^3$ ; median particle size,  $D_{50} = 2.0 \mu\text{m}$ ; minimum void ratio,  $e_{\text{min}} = 0.67$ ; and maximum void ratio,  $e_{\text{max}} = 1.17$ . Cylindrical specimens, 36 mm in diameter and 72 mm high, were compacted at a water content of 14 %, and the void ratio was 0.85. For the specimen preparation, the under-compaction technique (Ladd 1978) was used to ensure the specimen’s homogeneity. The SWRC was determined for the material using the filter paper technique. The filter paper tests were performed on the specimens of silt compacted at the water content and void ratio similar to the specimens that were used for element scale testing based on ASTM D5298-16. The SWRC data is presented in Figure 1(a). The van Genuchten’s (1981) fitted curve was also presented in this figure.

### 2.2 The resonant column torsional shear test device

A combined fixed-free Stokoe-type resonant column torsional shear (RCTS) test device was designed and constructed at Sharif University of Technology for the measurement of dynamic properties of soils under varying hydro-mechanical loading conditions. A schematic of the setup is presented in Figure 2.

In this test, a cylindrical soil specimen with a diameter of 36 mm and height of 72 mm is placed on top of a pedestal in good contact with a saturated high air-entry ceramic disk. The

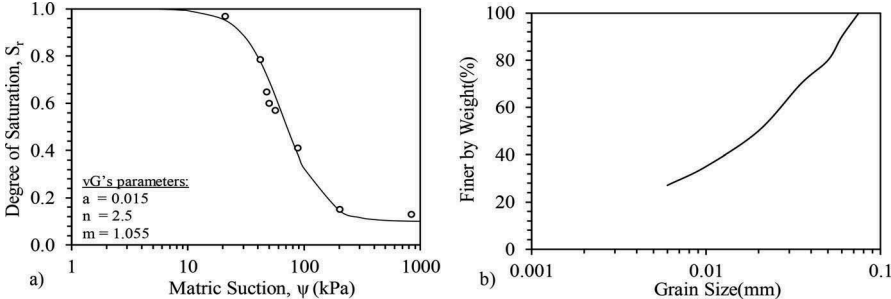


Figure 1. a) SWRC curve for non-plastic silt b) Grain-size distribution of non-plastic silt

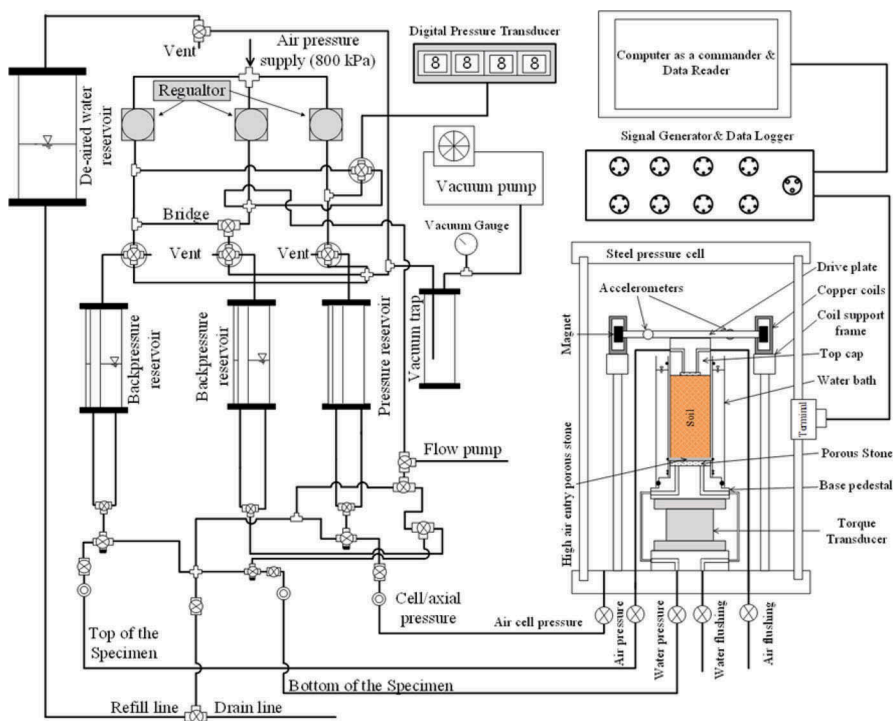


Figure 2. Resonant-column torsional shear setup

torsional force is applied through a non-contact electromagnetic driving system mounted on top of the specimen. The driving system consists of four permanent magnets, each housed within a pair of copper coil loops having opposite polarities. Application of an electrical current through the coils generates a magnetic field which imposes a force on the magnet, inducing a torque on the specimen through the drive plate.

In the resonant column test, a swept sine signal with constant amplitude is supplied to the copper coils using a dynamic signal generator. The range of frequency provided by this system is up to 1 kHz. Unlike traditional soil mechanics tests, in which a stress is applied to a specimen and strain is measured, in this test, the frequency of the imposed current is varied to identify the frequency at which the specimen reaches resonance. The resonant frequency is then measured using a pair of accelerometers connected to the top platen on top of the specimen. The accelerometers were built and developed at Sharif University with fixed voltage sensitivity, a force measurement range up to 18g peak, and a frequency range from 0.1 to 1000 Hz, which made them a suitable choice for this particular application.

The torsional shear includes three system components: a displacement transducer, a torque transducer, and a data logger. The displacement transducer is used to measure the movement of the drive plate. With an accuracy of 1  $\mu\text{m}$ , it allows tracking and measurement of strain at different levels from small to large. A non-rotary torque transducer with a torque capacity of 4.903 N.m is placed under the base pedestal to measure torque associated with torsional shear testing. During the test, a slow cyclic torsional loading with a 1 Hz frequency is applied to the specimen through the non-contact electromagnetic system on top of the specimen. The torque and displacement are then measured simultaneously using the displacement and torque transducers. These values are later used for the measurement of large-strain shear modulus and damping ratio under different loading conditions.

To protect the non-submersible electronic equipment, air pressure was used in this setup as the cell pressure, and the matric suction component of the unsaturated stress state was controlled using the axis translation technique. An approach was used in this study to implement

the axis-translation in a conventional RCTS test device without major modification. Specifically, a saturated high air entry ceramic disc having an air-entry suction of 300 kPa was embedded in the bottom platen to permit independent application (or measurement) of pore water pressure at the boundary of the soil specimen. To prevent stress concentrations beneath the disc, a traditional coarse porous stone was embedded in the bottom platen underneath the disc. During testing, a pressure panel connected to the specimen at the top and lower platen of the cell was used to apply pressure to the air and water phases to impose a suction value equal to  $u_a - u_w$  ( $u_a$  is the air pressure  $u_w$  is the water pressure). During this process, the water pressure was maintained constant while air pressure was changed to reach the desired suction level. The difference in pressure at the bottom (water) and at the top (air) of the specimen was measured using a differential pressure transducer connected to the bottom of the specimen. Water flow from the specimen during the saturated and unsaturated processes was measured using visual observation of water levels in graduated burettes of the pressure panel connected to the water drainage lines from the specimen and the chamber. These water flow measurements were later used to obtain changes in the degree of saturation and the void ratio of the specimen during loading. The tests were performed under backpressure saturation, which permits accurate outflow measurements using visual observations. A water bath was also mounted around the specimen to avoid diffusion of air from the cell into the membrane.

### 2.3 Testing procedure

The dynamic shear modulus and damping ratio of the material were determined under saturated and unsaturated conditions using the unsaturated resonant column torsional shear (RCTS) test device. As mentioned, RCTS test applies shear stress to a cylindrical soil specimen by the application of a cyclic rotational torque, which leads to a radial distribution in the magnitude of shear stress in the specimen.

After preparing the specimen and placing it on top of the bottom platen, the test was initiated by saturating the soil specimen using the backpressure technique under a constant confining pressure. During the saturation process, the cell pressure was first increased to 100 kPa and the backpressure was increased to 50 kPa, corresponding to an initial mean effective stress of 50 kPa. The cell pressure and water pressures applied to the top and bottom of the specimen were then increased in stages to 300 kPa and 250 kPa, respectively, maintaining an effective stress equal to 50 kPa. A minimum Skempton's B-value of 0.95 was observed for the tests presented in this paper. After saturation, the cell pressure was increased to reach an effective confining pressure of 300 kPa. After consolidation, air under the same pressure as the water backpressure (250 kPa) was flushed through all drainage lines connected to the top of the specimen. At this point, the initial effective confining pressure was equal to the net confining pressure, and this value was held constant through the rest of the test. Desaturation was then initiated by decreasing water pressure at the bottom, while maintaining a constant air pressure at the top of the specimen, and continued until the target matric suction was achieved. Shear modulus and damping ratio are heavily strain dependent. Therefore, the unsaturated tests were conducted on the specimen at three different strain levels using either resonant column (for small and medium strain levels) or torsional shear test (for large strain level) according to ASTM D4015 and ASTM D5311, respectively. The strain level in small, medium and large strain tests were around  $10^{-5}$ ,  $10^{-4}$ , and  $10^{-3}$ , respectively.

In the resonant column test, a swept sine signal with constant amplitude supplied by the dynamic signal generator was applied to the specimen and the resonant frequency was measured using the accelerometers attached to the top platen. Then, the resonant frequency along with soil density was used to determine the small strain shear modulus using Equation 1:

$$G_{max} = \rho V_s^2 \quad (1)$$

where  $\rho$  and  $V_s$  are the density and shear velocity of the specimen. The minimum damping ratio of the specimen was obtained using the half-power bandwidth method (Stokoe et al.

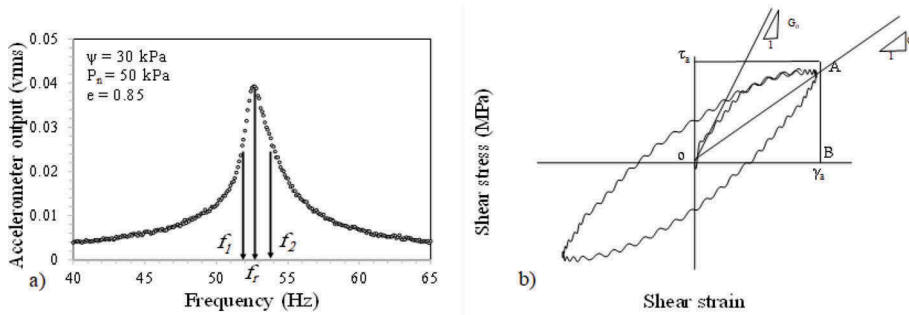


Figure 3. a) resonant column test at the suction of 30 kPa. b) hysteresis loop from torsional shear test at the suction 200 KPa

1999), which is based on the measurement of the width of the dynamic response curve around the resonance peak. Figure 3(a) shows the procedure used to calculate damping ratio at small strains for the matric suction of 30 kPa.

Hysteretic shear stress-strain loop for the silty soil specimen obtained from the torsional shear tests with matric suction and mean net stress of 200 kPa and 50 kPa are presented in Figure 3(b). These loops were used to define the secant shear modulus,  $G$ , and damping ratio,  $D$ , as follows (Equations 2 and 3):

$$G = \frac{\tau_a}{\gamma_a} = \frac{f(\gamma_a)}{\gamma_a} \tag{2}$$

$$D = \frac{1}{4\pi} \frac{\text{area of hysteresis loop}}{\text{area of triangle OAB}} \tag{3}$$

where  $\tau_a$  and  $\gamma_a$  denote the amplitudes of shear stress and shear strain, respectively,  $\Delta W$  is the energy dissipation per cycle represented by the area enclosed by the hysteresis loop, and  $W$  is the maximum stored energy equal to the area of the triangle bounded by a straight line defining the secant modulus.

### 3 EXPERIMENTAL RESULT AND DISCUSSION

To demonstrate the effect of matric suction or degree of saturation on shear modulus and damping ratio of unsaturated soils, a series of stress-controlled resonant column torsional shear tests was performed under three levels of matric suction (30, 80, and 200 kPa). The tests were performed at three different strain levels of  $10^{-5}$ ,  $10^{-4}$ , and  $10^{-3}$ . The shear modulus and shear strain were then calculated using the procedures presented in Figure 3.

#### 3.1 Effect of matric suction and shear strain

Figure 4(a) and (b) show the suction dependency of shear modulus and damping ratio at different strain levels. As shown in Figure 4, higher values of matric suction correspond to lower values of damping ratio and higher values of shear modulus, which implies that stronger interparticle bonding has been developed. This may be attributed to change in distribution of water due to the entrapped air bubbles, which may lead to different spatial impacts of air-water menisci on the interparticle connection in the soil specimen (Khalili and Zargarbashi, 2010). A significant influence of matric suction on damping ratio has been observed for large shear strain, which could be due to higher stiffness. Overall, this form of modulus variation is mostly in accordance with previously reported trends in small-strain shear modulus (Khosravi et al

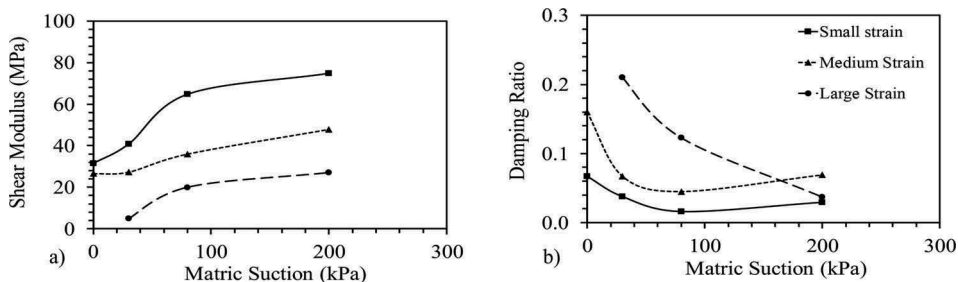


Figure 4. a) Shear modulus versus suction b) Damping ratio versus suction

2017, Ng et al 2009) and in large-strain shear modulus (Ghayoomi et al. 2017, Biglari et al. 2011) of unsaturated soils. Also, as expected, the shear strain increase resulted in a smaller shear modulus and a higher damping ratio regardless of the magnitude of the matric suction.

### 3.2 Normalized degradation curves

Hyperbolic models are frequently used in practice to represent nonlinear shear stress-shear strain behavior of soils in equivalent linear and nonlinear dynamic modeling problems. Several researchers have proposed shear modulus reduction ( $G/G_{max}$  versus  $\gamma$ ) curves that use the hyperbolic model as their basis, with parameters that fit the models to cyclic laboratory test results. Specifically, Darendeli (2001) proposed a form of hyperbolic model to determine the strain-dependent shear modulus of saturated soils, as follows:

$$\frac{G}{G_{max}} = \frac{1}{1 + \left(\frac{\gamma}{\gamma_r}\right)^a} \quad (4)$$

where  $\gamma_r$  is a reference strain (at which  $G/G_{max}$  is equal to 0.5), and  $a$  is a dimensionless exponent which varies with soil type (Stokoe et al., 1999, Darendeli, 2001). The experimental data that has been so far used to curve-fit these model coefficients mostly becomes sparse to saturated and dry soils. There is, however, very limited data for unsaturated soils. Therefore, models developed from such laboratory testing data sets require further information under different saturated and unsaturated conditions in order to provide accurate representation of shear strength and the corresponding nonlinear soil response.

In this study, the experimental data obtained from the unsaturated RCTS tests were used to calibrate the hyperbolic model proposed by Darendeli (2001) for unsaturated conditions. Figure 5 shows variations of the shear modulus,  $G$ , of the tested soil with shear strain,  $\gamma$ , at different matric suctions. As shown in this figure,  $G$  is presented in the normalized form with respect to  $G_{max}$ , i.e. in the customary  $G/G_{max}$  versus  $\gamma$ . Also, the curve of  $G/G_{max}$  proposed by Darendeli (2001) is presented. The model parameters  $\gamma_r$  and  $a$  were treated as fitting parameters in this study. As shown in Figure 5, the shear modulus reduction characteristics are relatively

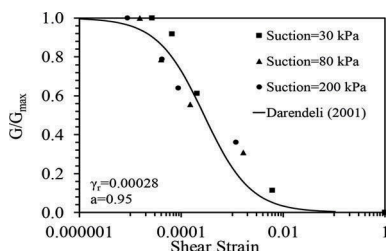


Figure 5. Normalized  $G/G_{max}$  curve for the specimens subjected to different suction values

independent of the matric suction. Also, a good agreement between the three sets of  $G/G_{max}$  data at different matric suctions and the curve obtained for saturated condition (Darendeli, 2001) is observed. Therefore, it can be concluded that Darendeli's hyperbolic model provides a fair representation of saturated and unsaturated shear strength at different levels of shear strain.

#### 4 CONCLUSION

A newly implemented resonant column torsional shear test device has proven suitable for testing unsaturated soils under suction-controlled condition via the axis-translation technique. Values of shear modulus and damping ratio at different strain levels and matric suctions were measured for the assessment of the dynamic properties of an unsaturated non-plastic silt. Results from the suction-controlled tests underscored the impact of matric suction on shear modulus and damping ratio. The results of this study indicated that an increase in the matric suction increases the shear modulus, while it decreases the damping ratio of soil. Also, the results of this study indicated that, provided that the model parameters are judiciously selected, the available model for saturated  $G/G_{max} - \gamma$  curves can accurately represent the unsaturated shear modulus.

#### REFERENCES

- Biglari, M & Jafari, M. K. & Shafiee, A & Mancuso, C & d'Onofrio, A. 2011. Shear Modulus and Damping Ratio of Unsaturated Kaolin Measured by New Suction-Controlled Cyclic Triaxial Device. *Geotechnical Testing Journal* Volume 34, Issue 5
- Darendeli, M. B. 2001. Development of a new family of normalized modulus reduction and material damping curves. *Ph.D. thesis, Univ. of Texas at Austin, Austin, TX.*
- Dong, Y., McCartney, J. S., and Lu, N. 2016. Small-strain shear modulus model for saturated and unsaturated soil. *Proc., Geo-Chicago 2016*, ASCE, Reston, VA, 316–325.
- Ghayoomi, M & Suprunenko, G and Mirshekari, M. 2017. Cyclic Triaxial Test to Measure Strain-Dependent Shear Modulus of Unsaturated Sand. *International Journal of Geomechanics* Volume 17, Issue 9
- Hall, J. R., Jr., & Richart, F. E., Jr. 1963. Dissipation of Elastic Wave Energy in Granular Soils. *Journal of the Soil Mechanics and Foundations Division*, ASCE, Vol. 89, No. SM6, Proc. Paper 3698, pp. 27–56.
- Hardin, B.O. & Black, W.L. 1969. Closure on vibration modulus of normally consolidated clay. *Journal of Soil Mechanics & Foundations Division*
- Hardin, B.O. & Drnevich, V.P. 1972. Shear modulus and damping in soils: Measurement and parameters effects. *Journal of Soil Mechanics & Foundations Division* Volume 98, Issue sm6
- Hilf, J.W. 1956. An investigation of pore-water pressure in compacted cohesive soils. *Ph.D. thesis, University of Colorado, Boulder.*
- Hoyos, L. R. & Suescún-Florez, E. A. & Puppala, A. J. 2015. Stiffness of intermediate unsaturated soil from simultaneous suction-controlled resonant column and bender element testing. *Engineering Geology*. Volume 188.
- Khalili, N & Zargarbashi, S. 2010. Influence of hydraulic hysteresis on effective stress in unsaturated soils. *Geotechnique* Volume 60, Issue 9
- Khosravi, A & Ghayoomi, M & McCartney, J.S. & Ko, H.Y., 2010, Impact of effective stress on the dynamic shear modulus of unsaturated sand, *GeoFlorida 2010: Advances in Analysis, Modeling & Design* page 410–419
- Khosravi, A & McCartney, J.S. 2011. Resonant Column Test for Unsaturated Soils with Suction–Saturation Control. *Geotechnical Testing Journal* Volume 34, Issue 6
- Khosravi, A & McCartney, J.S. 2012. Impact of Hydraulic Hysteresis on the Small-Strain Shear Modulus of Low Plasticity Soils. *Journal of Geotechnical and Geoenvironmental Eng.* Volume 138, Issue 11.
- Khosravi, A & Gheibi, A & Rahimi, M. 2016. Impact of void ratio and state parameters on the small strain shear modulus of unsaturated soils. *Japanese Geotech. Society Special Pub.* Volume 2. Issue 4.
- Khosravi, A & Rahimi, M & Gheibi, A and Shahrabi, M.M. 2017. Impact of Plastic Compression on the Small Strain Shear Modulus of Unsaturated Silts. *International Journal of Geomechanics.*



- Khosravi, A & Shahbazan, P & Pak, A. 2018. Impact of hydraulic hysteresis on the small strain shear modulus of unsaturated sand, *Soils and Foundations*, V 58, 12, P 344-354
- Mancuso, C & Vassallo, R & d'Onofrio, A. 2002. Small strain behavior of a silty sand in controlled-suction resonant column torsional shear tests. *Canadian Geotechnical Journal*. Volume 39, number 1
- Ng, C.W.W. & Xu, J & Yung, S.Y. 2009. Effects of wetting–drying and stress ratio on anisotropic stiffness of an unsaturated soil at very small strains. *Canadian Geotechnical Journal* Volume 46, number 9
- Stokoe, K. H., II & Darendeli, M. B. & Andrus, R. D., Brown, L. T., 1999. Dynamic Soil Properties: Laboratory, Field and Correlation Studies. *Second International Conference on Earthquake Geotechnical Engineering*, Vol. 3, Lisbon, Portugal.
- van Genuchten, M.T. 1980. A closed-form equation for predicting the hydraulic conductivity of unsaturated soils. *Soil Science Society Am. Journal* 44, pp. 892–898.